

Double-click Stapled Peptides for Inhibiting Protein–Protein Interactions

K. SHARMA^a, D. L. KUNCIW^a, W. XU^b, M. M. WIEDMANN^a,
Y. WU^a, H. F. SORE^a, W. R. J. D. GALLOWAY^a, Y. H. LAU^a,
L. S. ITZHAKI^b AND D. R. SPRING^{*a}

^aUniversity of Cambridge, Department of Chemistry, Lensfield Road, Cambridge, CB2 1EW, UK; ^bUniversity of Cambridge, Department of Pharmacology, Tennis Court Road, Cambridge, CB2 1PD, UK
*E-mail: spring@ch.cam.ac.uk

8.1 Introduction

Protein–protein interactions describe the biochemical events during which a protein’s activity and function are modulated by one or more separate interacting proteins. PPIs lead to measurable effects such as altering the kinetic properties of enzymes, allowing for substrate channeling, changing between active and inactive conformations, creating new binding sites, or serving as regulators in upstream or downstream events.¹ Complex networks of PPIs are intrinsic to most cellular functions of living organisms, and abnormal behavior of these proteins is often correlated with the commencement of various human diseases, like cancer.² Therefore, numerous studies have been carried out to assess the therapeutic potential of this target class and to discover novel PPI inhibitors.

PPI contact surfaces are often large (approximately 1500–3000 Å²) compared to those of protein–small molecule interactions (approximately 300–1000 Å²), and PPI interaction surfaces are usually flat and lack the grooves and pockets of proteins, which engage in small molecule binding.³ Due to the aforementioned reasons, twenty years ago PPIs were considered to be “undruggable”.⁴ Over the past two decades, there has been a considerable amount of research in this area and a number of different approaches have been reported for inhibiting PPIs.⁵ One such approach is peptidomimetics, which utilizes molecules designed to mimic the three-dimensional structure of peptides or proteins, while having the ability to interact with the biological target in the same way as the natural peptide or protein from which their structure was derived. While native peptides provide an accessible starting point for the design of peptidomimetics, peptides in isolation are poor contenders. On their own, short peptides often do not retain their native conformation, and hence binding capability, as there is a lack of structure inherently provided by the rest of the protein. Additionally, peptides are susceptible to rapid proteolysis and often suffer from poor cell permeability.

Many studies have focused on cyclic peptides as competitive inhibitors of PPIs as they are capable of selectively mimicking the protein contact.⁶ There are many effective peptidomimetic strategies described in the literature.^{7–9} In particular, stapled peptides, pioneered by Grubbs,¹⁰ Verdine,¹¹ Walensky,¹² and Sawyer,¹³ present a promising strategy to target “undruggable” therapeutic targets. Stapling as a form of macrocyclization refers to the process in which certain amino acid side chains of a peptide are covalently bonded for the stabilization of often, but not exclusively, α -helical structures in short peptide sequences.¹⁴ In theory, if the resultant length, position, and characteristics of the staple are optimal, the problems with short peptides in isolation may be overcome and binding affinity restored. Stapling can reinforce α -helical secondary structures if the non-native amino acids are positioned specifically on the same face of the helix, such as $i, i + 4$ and $i, i + 7$ ¹⁵ residues, or simply provide a means of macrocyclization for unstructured peptides. There are two general approaches: one-component and two-component stapling techniques. Whilst one-component stapling involves the direct linking of amino acid side chains, two-component stapling requires the use of a separate bi-functional linker to bridge the side chains of two non-proteogenic amino acids (Figure 8.1).

One-component stapling was the first to be proposed, starting with macrocyclization by lactamization *via* the incorporation of proteogenic amino acids Lys and Glu/Asp.¹⁷ Seminal work on hydrocarbon stapling by Grubbs and Blackwell led to the use of ring-closing metathesis as a method of stapling utilizing olefin-bearing amino acids.¹⁰ Other techniques include the reversible formation of disulfide bonds between two enantiomeric Cys residues,¹⁸ the use of an alkyne-bearing side chain and an azide-containing side chain for macrocyclization by Cu(I)-catalyzed azide–alkyne cycloaddition (CuAAC),¹⁹ and the formation of thioether bridges *via* a covalent linkage between Cys and α -bromo amide side chains.²⁰

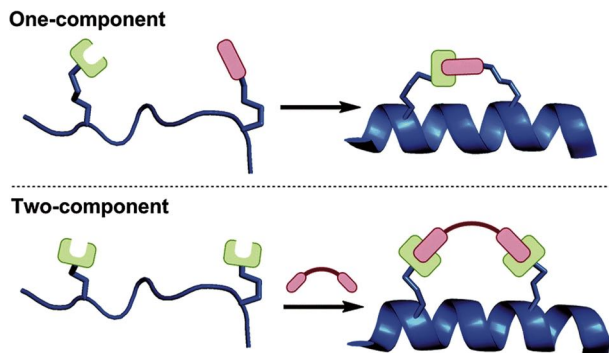
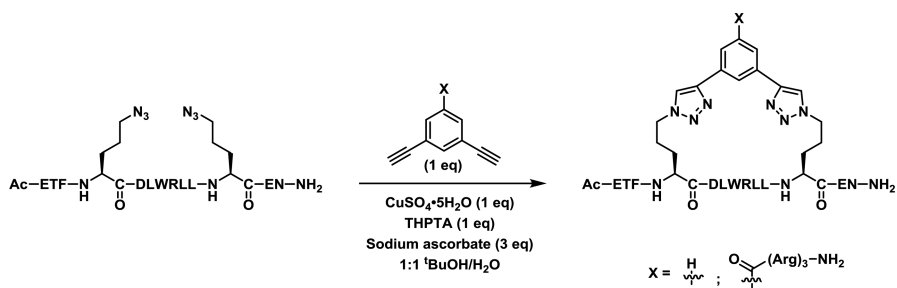


Figure 8.1 One- and two-component stapling techniques. Reproduced from ref. 16 with permission from The Royal Society of Chemistry.



Scheme 8.1 Cu(I)-catalyzed double-click peptide stapling. Reproduced from ref. 16 with permission from The Royal Society of Chemistry.

Two-component stapling relies on two steps: the intermolecular coupling of the bifunctional linker and peptide followed by an intramolecular coupling to complete the cyclization. An alternative, competing pathway, which is not possible in one-component stapling, results in double addition of the linker forming a linear peptide. Advances in this area have led to coping mechanisms such as conformational preorganization, varying the reacting side chain positions, and dilutions.¹⁶ Despite this complication, there are many advantages of two-component stapling, such as the ability to incorporate diverse staple linkages efficiently without the need to synthesize complex side chain-bearing amino acids for use in solid phase peptide synthesis (spps).

The Spring Group have devised a two-component stapling strategy termed the “double-click” approach to peptide stapling (Scheme 8.1).²¹ The approach is based on the robust nature of CuAAC, the archetypal click reaction reported by Sharpless²² and Meldal²³ and based on the original 1,3-dipolar cycloaddition developed by Huisgen.²⁴ This technique calls for the incorporation of two non-proteogenic azido amino acids into the peptide sequence of interest. Dialkynyl linkers then allow the formation of bistriazole-containing

macrocyclized peptides.²⁵ A large variety of stapled peptides can be synthesized by reacting the linear peptide with a library of dialkynyl linkers in a divergent manner. Furthermore, the required azido amino acids are easy to synthesize and are compatible with Fmoc chemistry and can be incorporated into the peptide chain *via* regular Merrifield spps.²⁶ In addition, the azide functionality allows chemospecific reactions and is tolerant to many other functional groups.

The remainder of this chapter will focus on the work of the Spring Group in the area of two-component “double-click” stapling, specifically:

- Efficient synthesis of Fmoc-protected azido amino acids.
- Optimization of the peptide sequence and use of functionalized staple linkages to modulate the cellular activity of stapled peptides.
- Metal-free strain-promoted peptide stapling.
- The application of double stapling in targeting the substrate-recognition domain of tankyrase to antagonize Wnt signaling, and the transcription factor HNF1 β /Importin α PPI, by using constrained non- α -helical peptide inhibitors.

It is important to note that the stapling approach developed by the Spring group has been used not only to constrain near-native peptidomimetics into α -helices as in the p53/MDM2 PPI, but also to provide the benefits of macrocyclization to unstructured peptidomimetics to target Tankyrase/Wnt and the HNF1 β /Importin α PPI.

8.2 Non-proteogenic Amino Acid Synthesis

Non-proteogenic amino acids containing azide groups are known to be useful in the design of synthetic peptides and proteins as a biorthogonal handle allowing for further functionalization *via* Staudinger ligation or CuAAC reactions. Azido amino acids have been used previously for the synthesis of peptidomimetics including triazole-containing macrocycles *via* CuAAC.²⁷

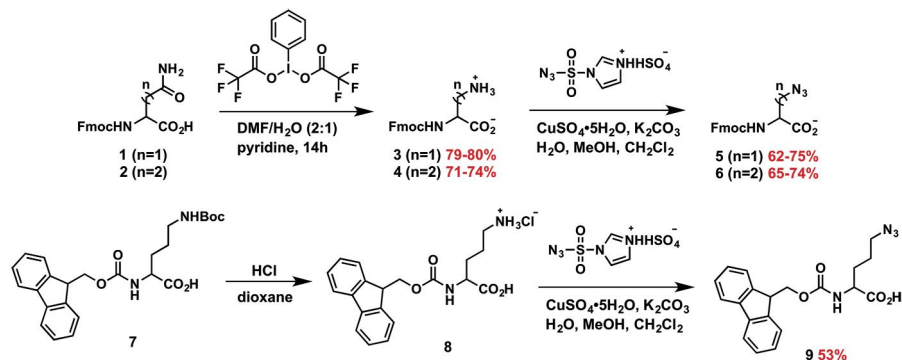
Since each coupling during spps requires multiple equivalents of pure amino acid, we sought to create a route to azido amino acids that was short, scalable, and high yielding, starting from inexpensive, commercially available compounds. Although there are existing literature procedures^{27–30} for the synthesis of azido amino acids, we decided to use copper-catalyzed diazotransfer chemistry to design a more straightforward and atom-efficient pathway.

To this end, amine bearing precursors, such as Fmoc-Dap[†]-OH (**3**), Fmoc-Dab[‡]-OH (**4**), and Fmoc-Orn[§]-OH (**8**), were prepared. Primary amines **3** and **4** were synthesized *via* Hofmann rearrangement of readily available

[†]Dap = 2,3-diaminopropionic acid.

[‡]Dab = 2,4-diaminobutyric acid.

[§]Orn = Ornithine.



Scheme 8.2 Synthesis of Fmoc-protected azido amino acids. Reproduced from Y. H. Lau and D. R. Spring, *Synlett*, 2011, 1917–1919³² with permission from Thieme; Copyright © 2011 Georg Thieme Verlag KG.

amino acids **1** and **2** (Scheme 8.2). Fmoc-Orn-OH (**8**) was synthesized *via* the acid deprotection of Fmoc-Orn(Boc)-OH (**7**). Imidazole-1-sulfonyl azide hydrochloride was chosen as the diazotransfer reagent as it is relatively less explosive than triflyl azide, its synthesis is scalable, and it is stable over the long term when stored at 4 °C.³¹

From the primary amines and the diazotransfer reagent, a route was developed using a biphasic solvent mixture of H₂O, MeOH, and CH₂Cl₂ adjusted to pH 9 with potassium carbonate to afford the azido amino acid **9** *via* CuAAC in relatively high yields. The synthesis can be performed on multigram scale with >98% chromatographic purity following an aqueous workup.³² This work serves as the sturdy foundation of all our experiments.

8.3 Peptide Sequence Optimization and Use of Functionalized Staple Linkages for Modulating the Cellular Activity of Stapled Peptides

By applying the double-click stapling concept to the p53/MDM2 interaction, a validated target for anticancer therapeutics, it was shown that Pro-27 replacement by the staple is the most suitable position (**P1**, Figure 8.2a)[¶] and Orn(N₃) is the ideal side chain length to attain optimal binding affinity (3.21 ± 0.38 nM) and cellular activity, when stapled with linker **10** (**P1–10**).³³ Substituting Orn(N₃) with Aha and Lys(N₃) as the side chain led to a decrease in the binding affinity of the stapled peptide to 10.5 ± 0.76 nM (**P9–10**) and 9.63 ± 0.87 nM (**P10–10**), respectively. Moreover, it was observed that activity could be induced in an otherwise impermeable p53 stapled peptide by incorporating a tri-arginine motif (**11**) on the staple linkage, rather than adjusting the peptide sequence (Figure 8.2a).³⁴ A series of linear aliphatic staples (**12–14**)

[¶]Aha = Azidohomoalanine; Lys = Lysine.

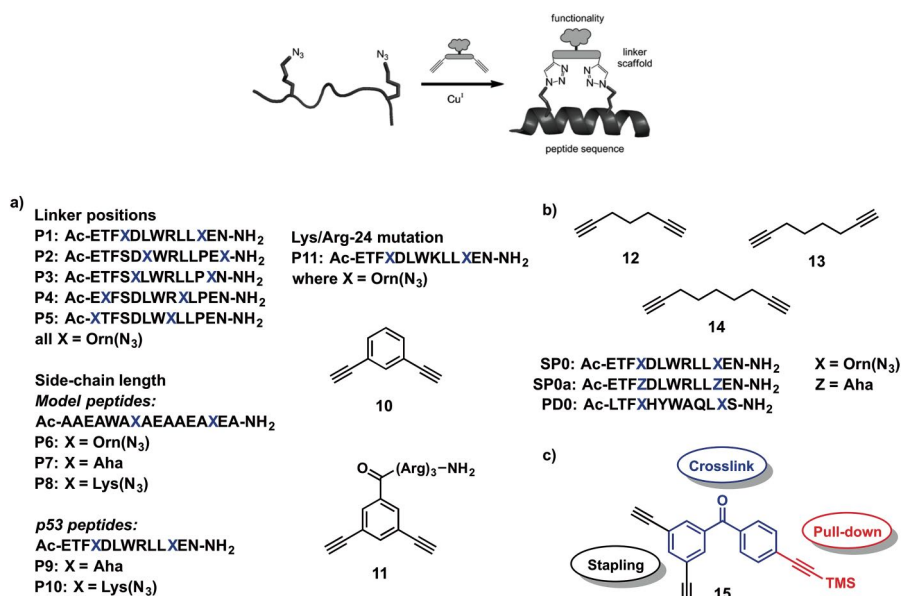


Figure 8.2 (a) Diazido peptides for stapling with dialkyne linkers **10** and **11** (reproduced from ref. 33 with permission from The Royal Society of Chemistry). (b) Linear aliphatic dialkyne linkers (from Y. H. Lau, P. de Andrade, G. J. McKenzie, A. R. Venkitaraman and D. R. Spring, Linear Aliphatic Dialkynes as Alternative Linkers for Double-Click Stapling of p53-Derived Peptides,²⁵ John Wiley and Sons, Copyright © 2014 by John Wiley & Sons, Inc.). (c) A multifunctional linker for peptide stapling and photoaffinity labelling (from Yuteng Wu, Lasse B. Olsen, Yu Heng Lau, Claus Hatt Jensen, Maxim Rossmann, Ysobel R. Baker, Hannah F. Sore, Súil Collins, David R. Spring, Development of a Multifunctional Benzophenone Linker for Peptide Stapling and Photoaffinity Labelling, John Wiley and Sons,³⁶ Copyright © 2016 by John Wiley & Sons, Inc.).

that complement the aromatic linkers were also developed.²⁵ Optimization of the combination of staple and sequence suggested that the aliphatic scaffolds can lead to enhanced binding *in vitro* and superior p53 activation in cells when combined with a phage-display-derived³⁵ sequence **PD0** (Figure 8.2b). The results suggest that different staple linkages can lead to very different peptide bioactivity in cells.

A benzophenone moiety was also incorporated into our dialkyne linker for photo-cross-linking. This novel multifunctional linker, **15**, serves as both a peptide stapling reagent and a photoaffinity probe with pulldown potential (Figure 8.2c).³⁶ The linker **15** can be accessed in four steps and the TMS group was conveniently removed under click conditions to reveal the terminal alkyne. Subsequent reaction with a biotinylated azide demonstrated its pulldown capability. As a proof of concept, this methodology was applied to a p53-derived peptide, which was effectively cross-linked with MDM2 after

UV irradiation. Current work is underway to extend this strategy to MDM2 labelling and pulldown in cell lysates or live cells, as well as applying it to study other PPIs.

8.4 Metal-free Strain-promoted Peptide Stapling

In 2003, Carolyn Bertozzi founded the field of bioorthogonal chemistry, involving reactions that can occur inside of living systems without interfering with native biochemical processes.³⁷ Despite the widespread utility of biorthogonal CuAAC reactions, their use inside living systems is limited due to the cytotoxicity of the Cu(I) catalyst involved (Figure 8.3a). *In vitro* and cell culture studies have demonstrated that metals like copper have the potential to cause oxidative damage to the cell and disrupt critical cellular functions.³⁸ Therefore, a copper-free click reaction was developed by Bertozzi in 2004, by utilizing a high-energy strained cyclooctyne molecule to increase the rate of reaction without the need for a catalyst.³⁹ As the ring strain of the cyclic molecule drives the click reaction forward, the reaction is also referred to as a strain-promoted azide–alkyne cycloaddition (SPAAC) (Figure 8.3b).³⁹

Since then, a number of strained molecules have been synthesized and applied to undergo metal-free click reactions *in vitro* and *in vivo*.⁴⁰ In 2002, Orita and co-workers^{41,42} reported the synthesis of strained Sondheimer–Wong diyne **16** by following a one-pot double-elimination protocol (Scheme 8.3).

This protocol was utilized by the Spring group to develop a metal-free double-click peptide stapling methodology (Scheme 8.4).⁴⁴ The double-click stapling of a p53-based diazidopeptide **17** with linker **16** in 1 : 1 ^tBuOH/H₂O gave stapled peptide **18** in 60% yield.

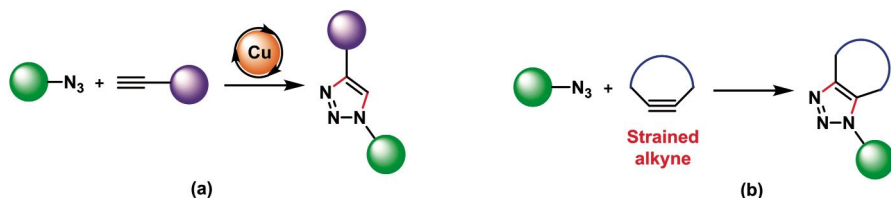
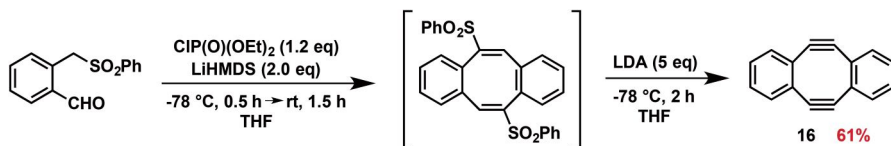
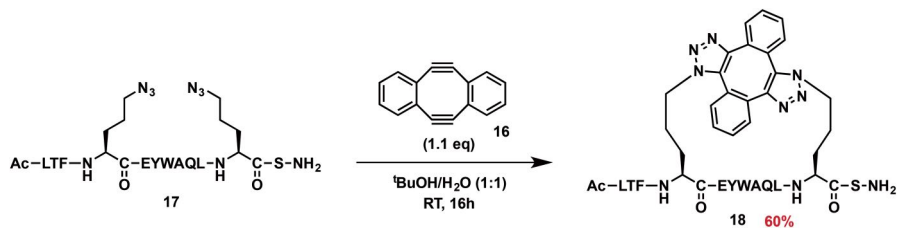


Figure 8.3 (a) General schematic of the Cu(I)-catalyzed click reaction by Sharpless and Meldal. (b) General schematic of the copper-free click reaction developed by Bertozzi.



Scheme 8.3 Orita's synthesis of a Sondheimer–Wong diyne. Reprinted with permission from ref. 42. Copyright (2014) American Chemical Society.



Scheme 8.4 Metal-free double-click peptide stapling.

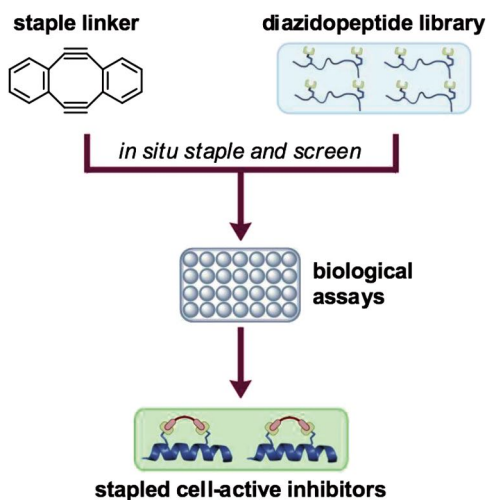


Figure 8.4 *In situ* strategy combining stapling and a primary biological assay in a single step.⁴⁴

HPLC analysis of the reaction mixture indicated that along with the major product **18**, there were other minor by-products with the same mass. These were suggested to be non-interchanging conformations of *syn* and *anti* regioisomers of the stapled peptide. Later on, X-ray crystallography studies on the MDM2-bound stapled peptide demonstrated the major isomer **18** to be the *anti*-regioisomer, which also confirmed the α -helical conformation of the stapled peptide. The stapled peptide **18** was found to be a potent helical inhibitor of the p53–MDM2 interaction. This methodology was extended to staple multiple MDM2-binding peptides in parallel, directly in the culture medium of a primary cell-based 96-well assay (Figure 8.4).⁴⁴ This *in situ* screening process led to the rapid selection of an optimal candidate with nanomolar binding affinity and enhanced proteolytic stability. This technique provides a faster way of screening a large peptide library avoiding the need to perform a separate stapling reaction for each peptide variant.

Two limitations of this stapling methodology are the poor water solubility of the linker leading to its precipitation during stapling, and the lack of

functional groups to which other motifs could be attached. Hence, current work is underway towards the synthesis of different heteroatom-substituted variants of the Sondheimer–Wong diyne **16**, with the aim of improving its solubility and providing a handle for further reactivity. Functionalization of the linker will hopefully also impart novel properties to the stapled peptide modifying its activity in cells and its binding affinity with MDM2.

8.5 Constrained Macrocyclic Non- α -helical Peptide Inhibitors

Peptide stapling to date has mainly focused on the stabilization of α -helical peptides^{11,12,45–47} and β -sheets.^{48–50} Generating mimetics of short peptide sequences that have no clear secondary structure prior to association with their binding partner is challenging,⁵¹ but has been achieved through macrocyclization and hence stabilization of the short peptides to give so-called constrained peptides. Constrained peptides can be synthesized through head-to-tail, head-to-side chain, side chain-to-tail or side chain-to-side chain cyclization (Figure 8.5).⁵²

Numerous examples of such macrocyclic peptides with high potency and cell permeability exist in nature,⁵³ such as cyclosporin A,^{52,54} antimicrobial polymyxins⁵⁵ and the hormone oxytocin.⁵⁶ In addition to mono-macrocyclic peptides, naturally occurring bicyclic peptides^{57–59} have inspired the synthesis of synthetic bicyclic drug compounds.^{60,61} Macrocyclization of these peptide sequences may be less efficient due to high conformational flexibility compared to α -helical peptides and there are no structure-based rules to follow (such as placing unnatural amino acids at i , $i + 4$ or $i + 7$ positions for stapling the same face of a helical turn),^{1,2} as every irregularly structured peptide is unique in its secondary structure when bound to the target protein. It is also difficult to predict the optimum linkage length for cross-linking such peptides, since computational approaches become less accurate in comparison to predictions for stapling α -helical peptides. Nevertheless, synthetic stapling or macrocyclization allows the peptides to be constrained in their bioactive conformation resulting in a lower entropic loss upon binding.⁶² Chemical modification of these irregularly structured peptides using

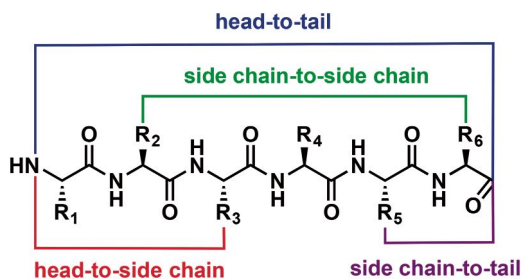


Figure 8.5 Peptide cyclization strategies.

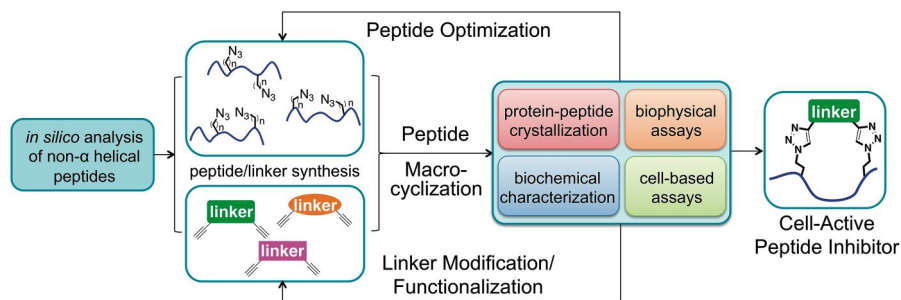


Figure 8.6 Design of constrained peptide inhibitors with a non- α -helical structure.

side chain-to-side chain double-click macrocyclization can potentially help to increase peptide stability towards proteasome-mediated degradation in cells, as well as their cell-penetrating capability. Using *in silico* analysis to scan through a peptide sequence for potential macrocyclization positions can minimize the number of peptides and linkers to be synthesized, and following a rational approach to improve the macrocyclic peptides using the information gained from protein crystallography and screening assays can efficiently provide potential peptide inhibitors that are protease-resistant, highly selective and bioactive in cells (Figure 8.6).

8.5.1 Design of Macrocyclic Peptide Inhibitors to Target the Substrate-recognition Domain of Tankyrase and Antagonize Wnt Signaling

Tankyrase (TNKS) is an ankyrin repeat-containing protein with a catalytic poly(ADP-ribose) polymerase (PARP) domain (Figure 8.7).^{63,64} The ankyrin-repeat domain, known as an ankyrin repeat cluster (ARC), is responsible for substrate recognition,⁶⁵ whereas the PARP activity of TNKS proteins plays a key role in controlling the axin level, a concentration-determining component of the β -catenin destruction complex in Wnt signaling.^{66–68} It has been an attractive therapeutic target for regulating β -catenin in many Wnt-dependent cancers, such as colorectal cancer, gastric cancer, breast cancer, and hepatocellular carcinoma, where accumulation of β -catenin is often observed.^{69–77} Small molecules developed for PARP inhibition of TNKS proteins prevent the PARylation and thereby degradation of axin *via* the ubiquitin-proteasome system, and axin in turn promotes the activity of the destruction complex, which phosphorylates β -catenin for degradation. However, potential drug resistance and target-specificity of these small molecule inhibitors remain challenges in this field, as many other members of the PARP family share homology in the PARP domain.^{78–80} Peptide inhibitors that instead target the substrate-recognition domain of TNKS represent an alternative approach to intervene in Wnt signaling. An unstructured motif, REAGDGEE, recognized by the TNKS ARC domain was determined by Guettler *et al.*⁸¹ and provided

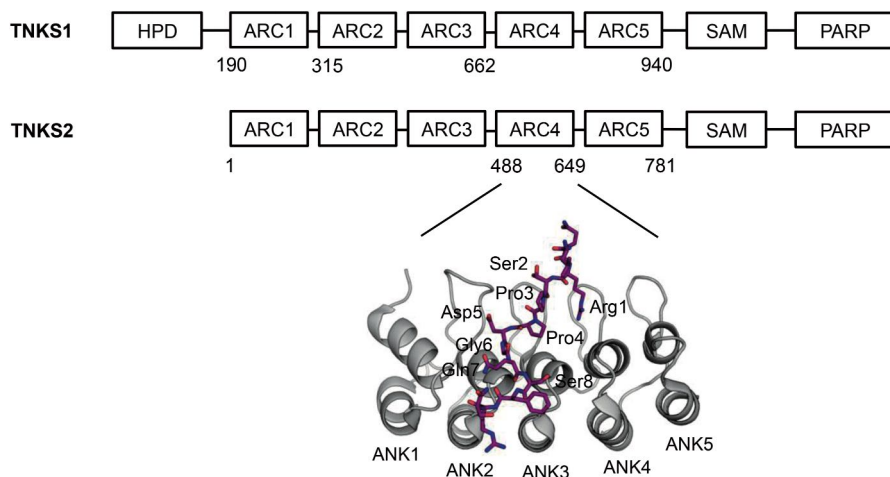
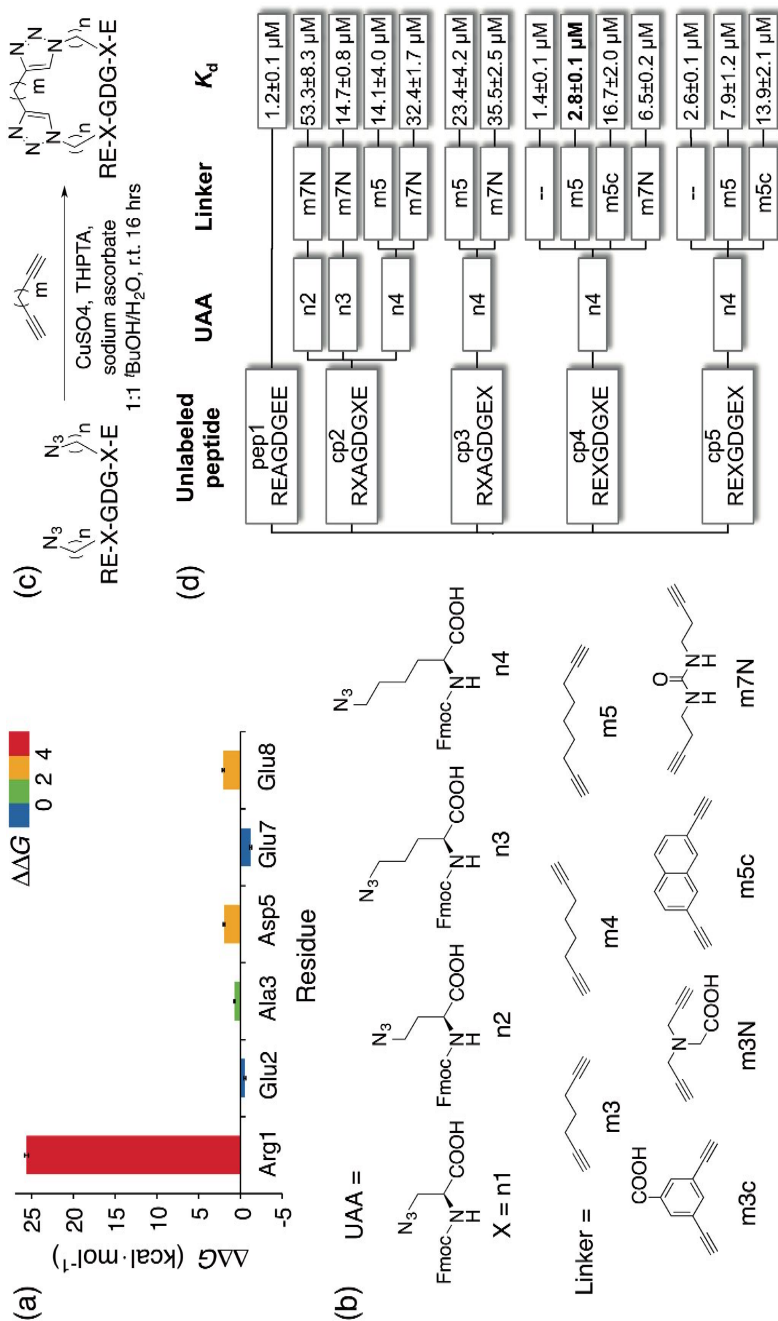


Figure 8.7 Domain architecture of TNKS1 and TNKS2, comprising a homopolymeric run of histidine, proline and serine (HPS) residues, the ankyrin repeat cluster (ARC), a sterile alpha motif (SAM), and catalytic PARP domains. The structure of human TNKS2 ARC4 (grey cartoon) is shown in complex with a substrate peptide LPHLQ**RSP**PDGQSF~~R~~S (purple; PDB ID: 3TWR);⁸¹ for clarity, only the central part of the peptide (in bold) is labelled. Adapted from Wenshu Xu, Yu Heng Lau, Gerhard Fischer, Yaw Sing Tan, Anasuya Chattopadhyay, Marc de la Roche, Marko Hyvönen, Chandra Verma, David R. Spring, and Laura S. Itzhaki, Macrocyclized Extended Peptides: Inhibiting the Substrate- Recognition Domain of Tankyrase, *The Journal of American Chemical Society*, 2017, **139**, 2245–2256,⁸² © 2017 American Chemical Society. Published under the terms of the CC BY 4.0 licence, <https://creativecommons.org/licenses/by/4.0/>.

the initial sequence basis for developing TNKS-specific peptide inhibitors to disrupt the TNKS–axin interaction in order to abolish the subsequent axin PARYlation. In this work, the two-component double-click strategy has been applied to macrocyclize the TNKS-binding peptides and lock their conformation in the active form, which is an extended, non-helical structure. The macrocyclized peptides showed enhanced binding affinities, proteolytic stability and cell permeability compared with the linear peptide, and one exhibited dose-dependent inhibition of Wnt signaling in cells.

One challenge for the initial macrocyclized peptide design was to determine the cross-linking positions in the sequence as the TNKS-binding peptides are non-helical and therefore the conventional rules for stapling α -helical peptides do not apply here. Computational alanine scanning was first carried out to assess which positions would be amenable to replacement by an azido-functionalized unnatural amino acid (UAA) in the consensus peptide (REAGDGEE, pep1 thereafter) without compromising the binding interaction with the ARC domain of TNKS (Figure 8.8a). Based on the *in silico* analysis, the first panel of peptides were synthesized, each with a pair of azido-functionalized UAAs (Figure 8.8b and d) at different positions in the


Figure 8.8

(a) Computational alanine scanning of consensus TNKS-binding peptide (REAGDGE) residues. $\Delta\Delta G$ for Ala3 was obtained by mutating it to glycine. Hot, warm, cool and cold spots are colored red, yellow, green and blue, respectively. (b) Unnatural amino acids (UAAs) and linkers used in the macrocyclized peptides. (c) Reaction scheme of the double-click chemistry on the extended TNKS-binding peptides. (d) The first panel of macrocyclized peptides; K_d values were obtained from competitive fluorescence polarization (FP). Adapted from Wenshu Xu, Yu Heng Lau, Gerhard Fischer, Yaw Sing Tan, Anasuya Chattopadhyay, Marc de la Roche, Marko Hyvönen, Chandra Verma, David R. Spring, and Laura S. Itzhaki, *Macrocyclized Extended Peptides: Inhibiting the Substrate- Recognition Domain of Tankyrase*, *The Journal of American Chemical Society*, 2017, **139**, 2245–2256,⁸² © 2017 American Chemical Society. Published under the terms of the CC BY 4.0 licence, <https://creativecommons.org/licenses/by/4.0/>.

sequence. The successful double-click reaction (Figure 8.8c) was confirmed by IR spectroscopy and high-resolution mass spectrometry, where only a single product was present where the two azide groups on the peptide reacted with one dialkynyl linker. From the first round of screening using a competitive fluorescence polarization (FP) assay, the sequence containing UAAs at positions 3 and 7 (cp4: REXGDGXE, where X stands for the UAA) was found to provide the highest binding affinity among the series (Figure 8.8d), and therefore this sequence was used for further optimizing the lengths of the UAA side chain, as well as the dialkynyl linker (Figure 8.8b).

To rationally improve the macrocyclic peptide for binding to the ARC domain of TNKS, the crystal structure of TNKS2 ARC4 in complex with a tight-binding macrocyclic peptide, cp4n4m5, was solved at 1.35 Å resolution (Figure 8.9b). The crystal structure suggested that the flexibility of the cross-linking allowed the peptide to adopt the same non-helical bioactive conformation as the linear peptide, though the lengths of the linker as well as the side chains of the UAAs could be shortened to provide more constraint and reduce the entropic cost during the binding. A second panel of macrocyclic peptides were then synthesized based on the optimal sequence cp4, in which the lengths of the side chain in the azido-functionalized UAAs and the dialkynyl linker were varied (Figure 8.9a and 8.8b). Two peptides, cp4n2m3 and cp4n2m3c, with shorter and more constrained cross-linking moieties were shown to bind more strongly than cp4n4m5 and also the linear pep1 to TNKS2 ARC4 in an FP assay (Figure 8.9a) and in isothermal titration calorimetry (ITC). The crystal structure of TNKS2 ARC4 in complex with the tight-binding cp4n2m3 (PDB ID: 5BXO) was subsequently solved at 1.33 Å resolution, confirming the design rationale that the smaller macrocycle size reduced the flexibility in the peptide and improved the binding affinity (Figure 8.9b). Similar to a stapled α -helical peptide, these macrocyclic peptides were shown to be much more resistant to proteolytic degradation than the linear peptide when treated with AspN peptidase, which cleaves between Gly–Asp of the sequence.

(peptide: cyan, linker: green) and cp4n4m5 (peptide: orange, linker: red). PDB IDs: 5BXO and 5BXU.⁸² (c) Chemical structure of the active peptide cp4n2m3c-Antp. (d) Confocal images of U2OS cells after incubation with 10 μ M of TAMRA-labelled peptides for 4 hours. Bar represents 10 μ m. The linker of cp4n2m3c-Arg, contains a polyarginine CPP and that of cp4n2m3c-Antp contains a penetratin peptide. (e) Dual-luciferase reporter assay showing the luciferase signal corresponding to the β -catenin level in Wnt3a-activated HEK 293T cells treated with a selection of unlabeled peptides. Macrocyclized CPP-conjugated cp4n2m3c-Antp showed dose-dependent inhibition of luciferase activity. Adapted from Wenshu Xu, Yu Heng Lau, Gerhard Fischer, Yaw Sing Tan, Anasuya Chattopadhyay, Marc de la Roche, Marko Hyvönen, Chandra Verma, David R. Spring, and Laura S. Itzhaki, Macrocyclized Extended Peptides: Inhibiting the Substrate- Recognition Domain of Tankyrase, *The Journal of American Chemical Society*, 2017, **139**, 2245–2256,⁸² © 2017 American Chemical Society. Published under the terms of the CC BY 4.0 licence, <https://creativecommons.org/licenses/by/4.0/>.

The cell-penetrating capabilities of the macrocyclic peptides were enhanced by coupling the linker to a selection of cell-penetrating peptides (CPPs); this did not disrupt the peptide–protein interaction because the cross-linking unit was pointing away from the protein surface according to the two crystal structures (Figure 8.9b) The CPP-conjugated macrocyclized peptides had significant cellular uptake even at 10 μM (Figure 8.9d) compared to the unconjugated macrocyclic peptides and the linear pep1. The unlabeled CPP-conjugated macrocyclic peptides did not exhibit any cytotoxicity at 100 μM . Treating HEK 293T cells in Wnt-activated conditions showed that cp4n2m3c-Antp, a macrocyclic TNKS-binding peptide conjugated with the penetratin sequence (Figure 8.9c), antagonized Wnt signaling by decreasing the β -catenin level in a dose-dependent manner (Figure 8.9e). This is the first example of a peptide inhibitor that directly targets the TNKS–axin binding interaction to antagonize Wnt signaling instead of blocking the catalytic PARP activity of TNKS. This proof-of-concept method provides guidance to develop future peptide inhibitors for TNKS in treating Wnt/ β -catenin-dependent cancers, and may overcome issues related to target-specificity and off-target effects of small molecule PARP inhibitors.⁸²

8.5.2 Development of Cell-permeable, Non-helical, Constrained Peptides to Target a Key Protein–Protein Interaction in Ovarian Cancer

Ovarian clear cell carcinoma (CCC) is a subtype of ovarian cancer.^{83,84} Prognosis for patients with advanced stage or relapsed disease is poor due to intrinsic resistance to platinum-based chemotherapy and the lack of targeted therapies for CCC.^{85,86} The development of novel, targeted therapeutics for CCC is therefore of high priority. Transcription factor HNF1 β is overexpressed in most, if not all, CCC cases^{87,88} and proliferation in CCC cell lines drops upon HNF1 β knockdown, caused by induced apoptotic cell death in CCC cells.⁸⁹ Drugs targeting HNF1 β have yet to be developed.

Human HNF1 β protein consists of 557 amino acids and a nuclear localization signal (NLS), which directs the nuclear import of the protein by interacting with structured binding sites on the nuclear import protein Importin α ,⁹⁰ is contained within the DNA-binding domain of HNF1 β .^{91–93}

Transcription factors are generally considered inferior drug targets,⁹⁴ but are highly attractive as key regulators of gene expression.^{95–97} Interestingly, 49% of transcription factor sequences consist of intrinsically disordered domains (IDDs).⁹⁸ Therapeutic targeting of the nuclear import of transcription factors provides a strategy for inhibiting transcription factor function, since activity depends on successful localization to the nucleus for transcription to take place.^{99,100} Competitive inhibition of the HNF1 β NLS–Importin α PPI by a constrained peptide inhibitor that is based on the HNF1 β NLS sequence may interfere with HNF1 β transcription factor function as shown in Figure 8.10. The self-inhibitory domain of Importin α binds to Importin β to free up the NLS-binding sites on Importin α . The constrained peptide

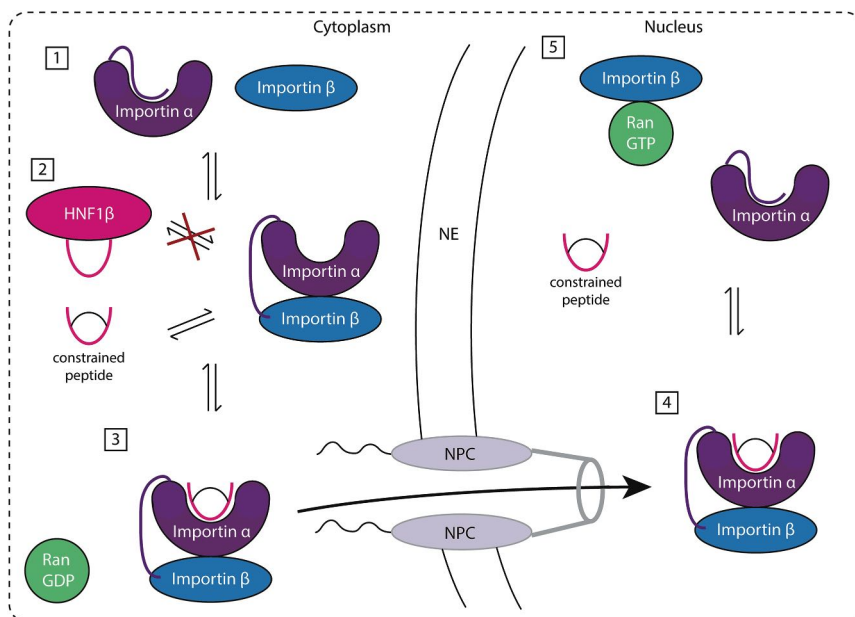


Figure 8.10 Targeting scheme of the nuclear import of transcription factor HNF1β with a constrained peptide inhibitor based on the NLS sequence. From Mareike M. Wiedmann, Yaw Sing Tan, Yuteng Wu, Shintaro Aibara, Wenshu Xu, Hannah F. Sore, Chandra S. Verma, Laura Itzhaki, Murray Stewart, James D. Brenton, David R. Spring, Development of Cell-Permeable, Non-Helical Constrained Peptides to Target a Key Protein–Protein Interaction in Ovarian Cancer,¹⁰¹ © 2016 The Authors. Published by Wiley-VCH Verlag GmbH & Co. KGaA. Published under the terms of the CC BY 4.0 licence, <https://creativecommons.org/licenses/by/4.0/>.

competes with the HNF1β protein for Importin α binding, which is in complex with Importin β in the cytoplasm. The trimer is imported through the nuclear pore complex (NPC) in the nuclear envelope (NE) into the nucleus, where it is released by RanGTP binding to Importin β.

The HNF1β NLS peptide, which is located in a flexible surface loop in between the two DNA-binding domains, was stapled to stabilize the NLS in its binding conformation. The crystal structure of the mImportin α1 ΔIBB with the HNF1β NLS peptide was determined and the HNF1β NLS peptide sequence was used as a starting point for constrained peptide design (Figure 8.11).

Three independently performed molecular dynamics (MD) simulations revealed the most important binding interactions of the HNF1β NLS peptide with two flanking residues on either side (1-TNKKMRRNRFK-11) with the mImportin α1 protein. Two discrepancies between the obtained crystal structure and the MD simulation results were identified. In the crystal structure, the backbone carbonyl group of Thr1 interacts with Arg238 on Importin α,

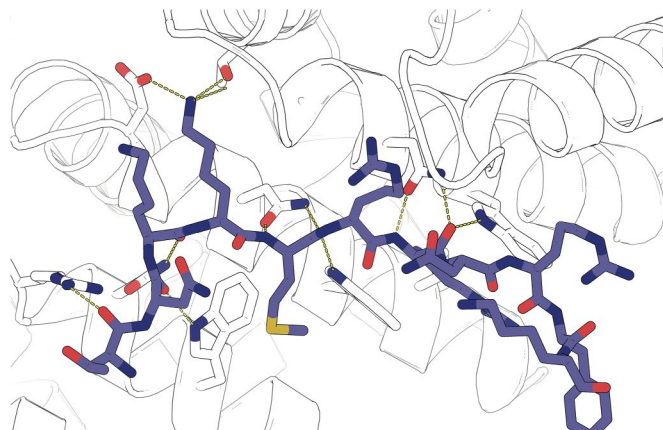


Figure 8.11 Crystal structure depicting interactions of the HNF1 β NLS peptide with mImportin α 1 with tryptophan stacking. Generated by Dr Shintaro Aibara and reprinted with kind permission.⁹³

whereas in two out of three MD simulations, this interaction is lost and H-bonding with Asp270 is observed instead (Figure 8.12A and B). Secondly, Arg9 forms a salt bridge with Glu465 on Importin α in the crystal structure, whereas a salt bridge with Glu107 was observed instead in all three MD simulations (Figure 8.12C and D). The results highlight the importance of using MD simulations to eliminate the effect of crystal packing and non-physiological contacts with neighboring proteins in the crystal, and to restore the protein structure in solution.¹⁰² In summary, the results suggest that residues Thr1 and Arg9 should be retained to maintain the binding potency of the constrained peptides.

The contribution of each HNF1 β NLS residue to the binding was then assessed by binding free energy decomposition.¹⁰³ Residues Phe10 and Lys11 contribute almost 0 kcal mol⁻¹ to the total binding free energy suggesting that they can be removed from the peptide with minimal disruption of the overall binding. Hence, the peptides are based on the following peptide sequence: 1-TNKKMRRNR-9. Computational alanine scanning on structures extracted from the MD simulations was then used to determine suitable stapling locations. Each residue was mutated to alanine and the difference in the binding free energy between mutant and wild-type was calculated, allowing the identification of residues that have little or negative contribution to the binding. The analysis revealed that Thr1, Lys4, Arg6, Arg7 and Arg9 are the most important residues for binding, whereas Asn2, Asn8, Phe10 and Lys11 only make negligible contributions to the binding. Since the staple is preferably placed on residues with side chains that have little or negative contribution to the binding, the staple may hence be placed at residues Asn2 and Asn8, Phe10, or Lys11 which contribute almost 0 kcal mol⁻¹ to the total binding free energy. Based on the obtained crystal structure (Figure 8.11), the staple is preferentially placed at residues Asn2 and Asn8 as

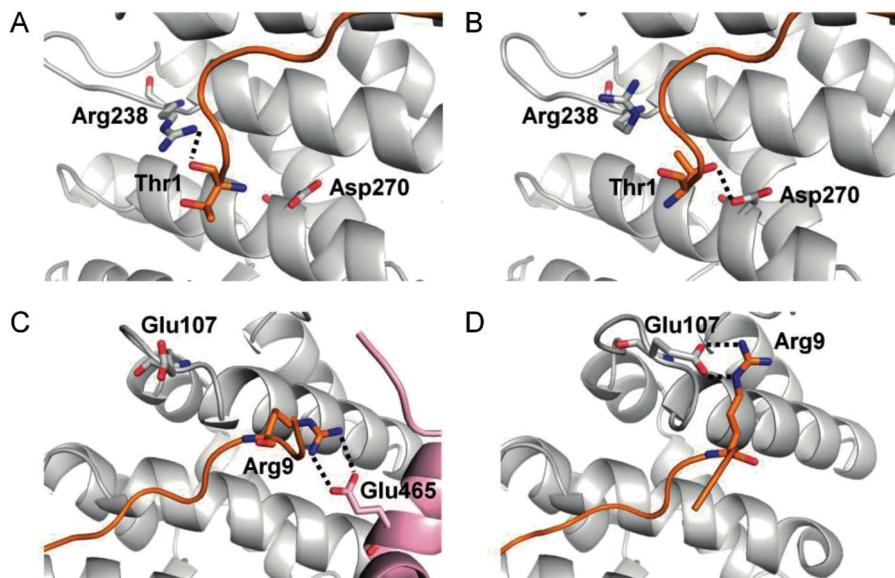


Figure 8.12 Binding interactions of the HNF1 β NLS peptide (orange) with mImportin α 1 (white) determined from X-ray crystallography and MD simulations. Trajectory structures shown are snapshots taken from the end of the simulations. (A) Backbone carbonyl oxygen of Thr1 hydrogen bonds with the side chain of Arg238 in the crystal structure. (B) Side chain of Thr1 hydrogen bonds with the side chain of Asp270 in the MD simulations. (C) Arg9 forms a salt bridge with Glu465 from a neighboring protein chain (pink) in the crystal structure. (D) Arg9 forms a salt bridge with Glu107 in the MD simulations. From Mareike M. Wiedmann, Yaw Sing Tan, Yuteng Wu, Shintaro Aibara, Wenshu Xu, Hannah F. Sore, Chandra S. Verma, Laura Itzhaki, Murray Stewart, James D. Brenton, David R. Spring, Development of Cell-Permeable, Non-Helical Constrained Peptides to Target a Key Protein–Protein Interaction in Ovarian Cancer,¹⁰¹ © 2016 The Authors. Published by Wiley-VCH Verlag GmbH & Co. KGaA. Published under the terms of the CC BY 4.0 licence, <https://creativecommons.org/licenses/by/4.0/>.

their side chains point towards each other in the bound peptide, to minimize constraint of the constrained peptide's bound conformation by the staple. The peptide sequence is therefore TAMRA-Ahx-²²⁷TX_nKKMRRX_nR²³⁵, with X_n referring to non-proteogenic azido amino acids used for stapling.

All linear peptides are synthesized using Fmoc-spps and then stapled using Cu(I)-click chemistry with three symmetrical dialkynyl linkers (Figure 8.13A and B). A direct fluorescence polarization assay is used to determine the binding constants. The dye, in this case TAMRA-5, reports a lower mobility of the dye-labelled ligand as it binds to the much heavier and hence less mobile protein, resulting in a higher degree of fluorescence polarization.¹⁰⁴ The linear HNF1 β NLS peptide sequence (Ac-TNKKMRRNRFK-NH₂) binds mImportin α 1 with a K_d of 1.7 μ M. TAMRA-5 alone binds mImportin α 1 with a

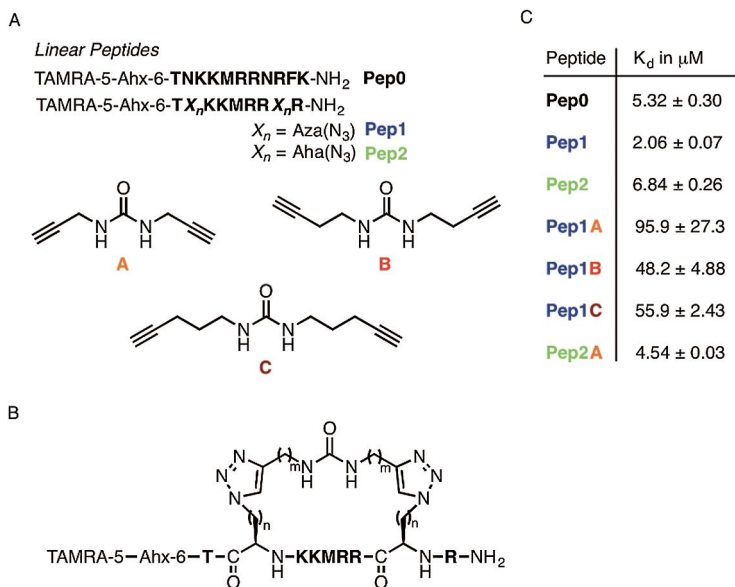


Figure 8.13 (A) Synthesized peptide sequences containing azido amino acids and linkers A–C. (B) General structure of bis-triazole constrained peptides with $n = 1$ or 2 and $m = 1–3$. (C) Direct FP assay binding affinities for (constrained) peptides in μM . From Mareike M. Wiedmann, Yaw Sing Tan, Yuteng Wu, Shintaro Aibara, Wenshu Xu, Hannah F. Sore, Chandra S. Verma, Laura Itzhaki, Murray Stewart, James D. Brenton, David R. Spring, Development of Cell-Permeable, Non-Helical Constrained Peptides to Target a Key Protein–Protein Interaction in Ovarian Cancer,¹⁰¹ © 2016 The Authors. Published by Wiley-VCH Verlag GmbH & Co. KGaA. Published under the terms of the CC BY 4.0 licence, <https://creativecommons.org/licenses/by/4.0/>.

K_d of approximately 125 μM , and is a useful control to establish if binding takes place *via* the peptide motif or is attributed to the dye. Compared to the linear wild-type peptide Pep0 there was a 2.5-fold improvement in the binding of Pep1. Constrained peptides Pep1A–Pep1C follow a rough trend with the binding affinity increasing with increasing linker length (Figure 8.13C). Constrained Pep2A bound with slightly improved binding affinity compared to linear peptide Pep0 and bound more tightly than its unconstrained precursor Pep2. This confirmed that an entropically-driven gain in binding affinity was achieved for Pep2A.

The cell permeability of the synthesized TAMRA-labelled linear and constrained peptides was assessed in the normal ovarian cell line IOSE4 using live-cell fluorescence microscopy. Pep1 and Pep2 displayed good cell permeability, which was retained upon stabilization (Pep1B, Pep2A). In conclusion, this work represents the first example of constraining an NLS peptide to target the nuclear import pathway. Further structural information on transcription factor HNF1 β binding to Importin α is required for the future design of Importin α isoform-selective inhibitors.

Acknowledgements

The Spring lab acknowledges support from the European Research Council under the European Union's Seventh Framework Programme (FP7/2007–2013)/ERC grant agreement no [279337/DOS]. In addition, the group research was supported by grants from the Engineering and Physical Sciences Research Council, Biotechnology and Biological Sciences Research Council, Medical Research Council, Royal Society and Wellcome Trust. LSI and WX acknowledge support from the Medical Research Council and the Medical Research Foundation.

References

1. E. M. Phizicky and S. Fields, *Microbiol. Rev.*, 1995, **59**, 94–123.
2. T. L. Nero, C. J. Morton, J. K. Holien, J. Wielens and M. W. Parker, *Nat. Rev. Cancer*, 2014, **14**, 248–262.
3. J. A. Wells and C. L. McClendon, *Nature*, 2007, **450**, 1001–1009.
4. G. L. Verdine and L. D. Walensky, *Clin. Cancer Res.*, 2007, **13**, 7264.
5. H. Yin and A. D. Hamilton, *Angew. Chem., Int. Ed.*, 2005, **44**, 4130–4163.
6. B. N. Bullock, A. L. Jochim and P. S. Arora, *J. Am. Chem. Soc.*, 2011, **133**, 14220–14223.
7. R. M. J. Liskamp, D. T. S. Rijkers, J. A. W. Kruijtzter and J. Kemmink, *ChemBioChem*, 2011, **12**, 1626–1653.
8. V. Azzarito, K. Long, N. S. Murphy and A. J. Wilson, *Nat. Chem.*, 2013, **5**, 161–173.
9. A. Grauer and B. König, *Eur. J. Org. Chem.*, 2009, **2009**, 5099–5111.
10. H. E. Blackwell and R. H. Grubbs, *Angew. Chem., Int. Ed.*, 1998, **37**, 3281–3284.
11. C. E. Schafmeister, J. Po and G. L. Verdine, *J. Am. Chem. Soc.*, 2000, **122**, 5891–5892.
12. L. D. Walensky, A. L. Kung, I. Escher, T. J. Malia, S. Barbuto, R. D. Wright, G. Wagner, G. L. Verdine and S. J. Korsmeyer, *Science*, 2004, **305**, 1466–1470.
13. Y. S. Chang, B. Graves, V. Guerlavais, C. Tovar, K. Packman, K.-H. To, K. A. Olson, K. Kesavan, P. Gangurde, A. Mukherjee, T. Baker, K. Darlak, C. Elkin, Z. Filipovic, F. Z. Qureshi, H. Cai, P. Berry, E. Feyfant, X. E. Shi, J. Horstick, D. A. Annis, A. M. Manning, N. Fotouhi, H. Nash, L. T. Vassilev and T. K. Sawyer, *Proc. Natl. Acad. Sci.*, 2013, **110**, E3445–E3454.
14. L. D. Walensky and G. H. Bird, *J. Med. Chem.*, 2014, **57**, 6275–6288.
15. O. Torres, D. Yüksel, M. Bernardina, K. Kumar and D. Bong, *ChemBioChem*, 2008, **9**, 1701–1705.
16. Y. H. Lau, P. de Andrade, Y. Wu and D. R. Spring, *Chem. Soc. Rev.*, 2015, **44**, 91–102.
17. A. M. Felix, E. P. Heimer, C.-T. Wang, T. J. Lambros, A. Fournier, T. F. Mowles, S. Maines, R. M. Campbell, B. B. Wegrzynski, V. Toome, D. Fry and V. S. Madison, *Int. J. Pept. Protein Res.*, 1988, **32**, 441–454.

18. D. Y. Jackson, D. S. King, J. Chmielewski, S. Singh and P. G. Schultz, *J. Am. Chem. Soc.*, 1991, **113**, 9391–9392.
19. J. E. Moses and A. D. Moorhouse, *Chem. Soc. Rev.*, 2007, **36**, 1249–1262.
20. F. M. Brunel and P. E. Dawson, *Chem. Commun.*, 2005, 2552–2554.
21. Y. H. Lau, Y. Wu, P. de Andrade, W. R. J. D. Galloway and D. R. Spring, *Nat. Protoc.*, 2015, **10**, 585–594.
22. V. V. Rostovtsev, L. G. Green, V. V. Fokin and K. B. Sharpless, *Angew. Chem., Int. Ed.*, 2002, **41**, 2596–2599.
23. C. W. Tornøe, C. Christensen and M. Meldal, *J. Org. Chem.*, 2002, **67**, 3057–3064.
24. R. Huisgen, *Proc. Chem. Soc.*, 1961, 357–396.
25. Y. H. Lau, P. de Andrade, G. J. McKenzie, A. R. Venkitaraman and D. R. Spring, *ChemBioChem*, 2014, **15**, 2680–2683.
26. R. B. Merrifield, *J. Am. Chem. Soc.*, 1963, **85**, 2149–2154.
27. M. Roice, I. Johannsen and M. Meldal, *QSAR Comb. Sci.*, 2004, **23**, 662–673.
28. S. I. van Kasteren, H. B. Kramer, H. H. Jensen, S. J. Campbell, J. Kirkpatrick, N. J. Oldham, D. C. Anthony and B. G. Davis, *Nature*, 2007, **446**, 1105–1109.
29. K. L. Kiick, E. Saxon, D. A. Tirrell and C. R. Bertozzi, *Proc. Natl. Acad. Sci.*, 2002, **99**, 19–24.
30. N. Miller, G. M. Williams and M. A. Brimble, *Org. Lett.*, 2009, **11**, 2409–2412.
31. E. D. Goddard-Borger and R. V. Stick, *Org. Lett.*, 2007, **9**, 3797–3800.
32. Y. H. Lau and D. R. Spring, *Synlett*, 2011, 1917–1919.
33. Y. H. Lau, P. de Andrade, N. Skold, G. J. McKenzie, A. R. Venkitaraman, C. Verma, D. P. Lane and D. R. Spring, *Org. Biomol. Chem.*, 2014, **12**, 4074–4077.
34. Y. H. Lau, P. de Andrade, S.-T. Quah, M. Rossmann, L. Laraia, N. Skold, T. J. Sum, P. J. E. Rowling, T. L. Joseph, C. Verma, M. Hyvonen, L. S. Itzhaki, A. R. Venkitaraman, C. J. Brown, D. P. Lane and D. R. Spring, *Chem. Sci.*, 2014, **5**, 1804–1809.
35. B. Hu, D. M. Gilkes and J. Chen, *Cancer Res.*, 2007, **67**, 8810.
36. Y. Wu, L. B. Olsen, Y. H. Lau, C. H. Jensen, M. Rossmann, Y. R. Baker, H. F. Sore, S. Collins and D. R. Spring, *ChemBioChem*, 2016, **17**, 689–692.
37. E. M. Sletten and C. R. Bertozzi, *Angew. Chem., Int. Ed.*, 2009, **48**, 6974–6998.
38. D. C. Kennedy, C. S. McKay, M. C. B. Legault, D. C. Danielson, J. A. Blake, A. F. Pegoraro, A. Stolow, Z. Mester and J. P. Pezacki, *J. Am. Chem. Soc.*, 2011, **133**, 17993–18001.
39. N. J. Agard, J. A. Prescher and C. R. Bertozzi, *J. Am. Chem. Soc.*, 2004, **126**, 15046–15047.
40. E. M. Sletten and C. R. Bertozzi, *Acc. Chem. Res.*, 2011, **44**, 666–676.
41. A. Orita, D. Hasegawa, T. Nakano and J. Otera, *Chem.–Eur. J.*, 2002, **8**, 2000–2004.

42. F. Xu, L. Peng, K. Shinohara, T. Morita, S. Yoshida, T. Hosoya, A. Orita and J. Otera, *J. Org. Chem.*, 2014, **79**, 11592–11608.
43. H. N. C. Wong, P. J. Garratt and F. Sondheimer, *J. Am. Chem. Soc.*, 1974, **96**, 5604–5605.
44. Y. H. Lau, Y. Wu, M. Rossmann, B. X. Tan, P. de Andrade, Y. S. Tan, C. Verma, G. J. McKenzie, A. R. Venkitaraman, M. Hyvönen and D. R. Spring, *Angew. Chem., Int. Ed.*, 2015, **54**, 15410–15413.
45. M. M. Madden, A. Muppidi, Z. Li, X. Li, J. Chen and Q. Lin, *Bioorg. Med. Chem. Lett.*, 2011, **21**, 1472–1475.
46. M. L. Stewart, E. Fire, A. E. Keating and L. D. Walensky, *Nat. Chem. Biol.*, 2010, **6**, 595–601.
47. K. Pitter, F. Bernal, J. LaBelle and L. D. Walensky, 2008, **446**, 387–408.
48. O. Khakshoor and J. S. Nowick, *Org. Lett.*, 2009, **11**, 3000–3003.
49. A. A. Virgilio and J. A. Ellman, *J. Am. Chem. Soc.*, 1994, **116**, 11580–11581.
50. A. A. Virgilio, S. C. Schürer and J. A. Ellman, *Tetrahedron Lett.*, 1996, **37**, 6961–6964.
51. D. E. Scott, A. R. Bayly, C. Abell and J. Skidmore, *Nat. Rev. Drug Discovery*, 2016, **15**, 533–550.
52. T. A. Hill, N. E. Shepherd, F. Diness and D. P. Fairlie, *Angew. Chem., Int. Ed. Engl.*, 2014, **53**, 13020–13041.
53. D. J. Craik, *Science*, 2006, **311**, 1563–1564.
54. D. Faulds, K. L. Goa and P. Benfield, *Drugs*, 1993, **45**, 953–1040.
55. T. Velkov, P. E. Thompson, R. L. Nation and J. Li, *J. Med. Chem.*, 2010, **53**, 1898–1916.
56. J. P. Rose, C.-K. Wu, C.-D. Hsiao, E. Breslow and B.-C. Wang, *Nat. Struct. Mol. Biol.*, 1996, **3**, 163–169.
57. S. D. Jolad, J. J. Hoffman, S. J. Torrance, R. M. Wiedhopf, J. R. Cole, S. K. Arora, R. B. Bates, R. L. Gargiulo and G. R. Kriek, *J. Am. Chem. Soc.*, 1977, **99**, 8040–8044.
58. M. Zalacain, E. Zaera, D. Vázquez and A. Jiménez, *FEBS Lett.*, 1982, **148**, 95–97.
59. D. A. Bushnell, P. Cramer and R. D. Kornberg, *Proc. Natl. Acad. Sci. U. S. A.*, 2002, **99**, 1218–1222.
60. A. Angelini, L. Cendron, S. Chen, J. Touati, G. Winter, G. Zanotti and C. Heinis, *ACS Chem. Biol.*, 2012, **7**, 817–821.
61. S. Chen, J. Morales-Sanfrutos, A. Angelini, B. Cutting and C. Heinis, *ChemBioChem*, 2012, **13**, 1032–1038.
62. J. S. McMurray, P. K. Mandal, W. S. Liao, J. Klostergaard and F. M. Robertson, *JAKSTAT*, 2012, **1**, 263–347.
63. H. Seimiya and S. Smith, *J. Biol. Chem.*, 2002, **277**, 14116–14126.
64. S. Smith, I. Gariat, A. Schmitt and T. de Lange, *Science*, 1998, **282**, 1484–1487.
65. J. I. Sbodio and N.-W. Chi, *J. Biol. Chem.*, 2002, **277**, 31887–31892.
66. S.-M. A. Huang, Y. M. Mishina, S. Liu, A. Cheung, F. Stegmeier, G. A. Michaud, O. Charlat, E. Wiellette, Y. Zhang, S. Wiessner, M. Hild, X. Shi,

- C. J. Wilson, C. Mickanin, V. Myer, A. Fazal, R. Tomlinson, F. Serluca, W. Shao, H. Cheng, M. Shultz, C. Rau, M. Schirle, J. Schlegl, S. Ghidelli, S. Fawell, C. Lu, D. Curtis, M. W. Kirschner, C. Lengauer, P. M. Finan, J. A. Tallarico, T. Bouwmeester, J. A. Porter, A. Bauer and F. Cong, *Nature*, 2009, **461**, 614–620.
67. S. Ikeda, S. Kishida, H. Yamamoto, H. Murai, S. Koyama and A. Kikuchi, *EMBO J.*, 1998, **17**, 1371–1384.
68. A. Salic, E. Lee, L. Mayer and M. W. Kirschner, *Mol. Cell*, 2000, **5**, 523–532.
69. O. Aguilera, M. F. Fraga, E. Ballestar, M. F. Paz, M. Herranz, J. Espada, J. M. Garcia, A. Munoz, M. Esteller and J. M. Gonzalez-Sancho, *Oncogene*, 2006, **25**, 4116–4121.
70. J. N. Anastas and R. T. Moon, *Nat. Rev. Cancer*, 2013, **13**, 11–26.
71. K. Breuhahn, T. Longerich and P. Schirmacher, *Oncogene*, 2006, **25**, 3787–3800.
72. H. Clevers and R. Nusse, *Cell*, 2012, **149**, 1192–1205.
73. G. J. Klarmann, A. Decker and W. L. Farrar, *Epigenetics*, 2008, **3**, 59–63.
74. M. Kurayoshi, N. Oue, H. Yamamoto, M. Kishida, A. Inoue, T. Asahara, W. Yasui and A. Kikuchi, *Cancer Res.*, 2006, **66**, 10439–10448.
75. P. Laurent-Puig and J. Zucman-Rossi, *Oncogene*, 2006, **25**, 3778–3786.
76. S. Y. Lin, W. Xia, J. C. Wang, K. Y. Kwong, B. Spohn, Y. Wen, R. G. Pestell and M. C. Hung, *Proc. Natl. Acad. Sci. U. S. A.*, 2000, **97**, 4262–4266.
77. P. J. Morin, A. B. Sparks, V. Korinek, N. Barker, H. Clevers, B. Vogelstein and K. W. Kinzler, *Science*, 1997, **275**, 1787–1790.
78. S. L. Edwards, R. Brough, C. J. Lord, R. Natrajan, R. Vatcheva, D. A. Levine, J. Boyd, J. S. Reis-Filho and A. Ashworth, *Nature*, 2008, **451**, 1111–1115.
79. C. J. Lord and A. Ashworth, *Curr. Opin. Pharmacol.*, 2008, **8**, 363–369.
80. M. Rouleau, A. Patel, M. J. Hendzel, S. H. Kaufmann and G. G. Poirier, *Nat. Rev. Cancer*, 2010, **10**, 293–301.
81. S. Guettler, J. LaRose, E. Petsalaki, G. Gish, A. Scotter, T. Pawson, R. Rottapel and F. Sicheri, *Cell*, 2011, **147**, 1340–1354.
82. W. Xu, Y. H. Lau, G. Fischer, Y. S. Tan, A. Chattopadhyay, M. de la Roche, M. Hyvönen, C. Verma, D. R. Spring and L. S. Itzhaki, *J. Am. Chem. Soc.*, 2017, **139**, 2245–2256.
83. S. Vaughan, J. I. Coward, R. C. Bast Jr, A. Berchuck, J. S. Berek, J. D. Brenton, G. Coukos, C. C. Crum, R. Drapkin, D. Etemadmoghadam, M. Friedlander, H. Gabra, S. B. Kaye, C. J. Lord, E. Lengyel, D. A. Levine, I. A. McNeish, U. Menon, G. B. Mills, K. P. Nephew, A. M. Oza, A. K. Sood, E. A. Stronach, H. Walczak, D. D. Bowtell and F. R. Balkwill, *Nat. Rev. Cancer*, 2011, **11**, 719–725.
84. H. Kobayashi, K. Sumimoto, N. Moniwa, M. Imai, K. Takakura, T. Kurokaki, E. Morioka, K. Arisawa and T. Terao, *Int. J. Gynecol. Cancer*, 2007, **17**, 37–43.
85. D. S. P. Tan and S. Kaye, *J. Clin. Pathol.*, 2007, **60**, 355–360.
86. D. S. Tan, R. E. Miller and S. B. Kaye, *Br. J. Cancer*, 2013, **108**, 1553–1559.
87. N. Kato, S. Sasou and T. Motoyama, *Mod. Pathol.*, 2006, **19**, 83–89.

88. K. Yamaguchi, M. Mandai, T. Oura, N. Matsumura, J. Hamanishi, T. Baba, S. Matsui, S. K. Murphy and I. Konishi, *Oncogene*, 2010, **29**, 1741–1752.
89. A. Tsuchiya, M. Sakamoto, J. Yasuda, M. Chuma, T. Ohta, M. Ohki, T. Yasugi, Y. Taketani and S. Hirohashi, *Am. J. Pathol.*, 2003, **163**, 2503–2512.
90. D. Calderon, W. D. Richardson, A. F. Markham and A. E. Smith, *Nature*, 1984, **311**, 33–38.
91. G. Wu, S. Bohn and G. U. Ryffel, *Eur. J. Biochem.*, 2004, **271**, 3715–3728.
92. S. Bohn, H. Thomas, G. Turan, S. Ellard, C. Bingham, A. T. Hattersley and G. U. Ryffel, *J. Am. Soc. Nephrol.*, 2003, **14**, 2033–2041.
93. M. M. Wiedmann, S. Aibara, D. R. Spring, M. Stewart and J. D. Brenton, *J. Struct. Biol.*, 2016, **195**, 273–281.
94. P. Imming, C. Sinning and A. Meyer, *Nat. Rev. Drug Discovery*, 2006, **5**, 821–834.
95. A. G. Papavassiliou and P. A. Konstantinopoulos, *J. Am. Med. Assoc.*, 2011, **305**, 2349–2350.
96. M. N. Patel, M. D. Halling-Brown, J. E. Tym, P. Workman and B. Al-Lazikani, *Nat. Rev. Drug Discovery*, 2013, **12**, 35–50.
97. F. Fontaine, J. Overman and M. François, *Cell Regener.*, 2015, **4**, 1–12.
98. Y. Minezaki, K. Homma, A. R. Kinjo and K. Nishikawa, *J. Mol. Biol.*, 2006, **359**, 1137–1149.
99. P. Ferrigno and P. A. Silver, *Oncogene*, 1999, **18**, 6129–6134.
100. A. Komeili and E. K. O’Shea, *Curr. Opin. Cell Biol.*, 2000, **12**, 355–360.
101. M. M. Wiedmann, Y. S. Tan, Y. Wu, S. Aibara, W. Xu, H. F. Sore, C. S. Verma, L. Itzhaki, M. Stewart, J. D. Brenton and D. R. Spring, *Angew. Chem., Int. Ed.*, 2017, **56**, 524–529.
102. T. Terada and A. Kidera, *J. Phys. Chem. B*, 2012, **116**, 6810–6818.
103. H. Gohlke, C. Kiel and D. A. Case, *J. Mol. Biol.*, 2003, **330**, 891–913.
104. J. R. Unruh, G. Gokulrangan, G. H. Lushington, C. K. Johnson and G. S. Wilson, *Biophys. J.*, 2005, **88**, 3455–3465.